

SOLE SENSE: Smart Haptic Navigation Footwear for Obstacle Detection and Environmental Hazard Awareness for Visually Impaired Users

G. Neelavathi, Hudson K. Siju, Elambarithi S, Harish R, Jeeva Prakash S

Department of Electronics and Communication Engineering, Mahendra Engineering College, Namakkal, Tamil Nadu, India

neelavathig@mahendra.info, sijuhudson@gmail.com, elangoelambarithi@gmail.com, harishhariss1313@gmail.com, sjeevaprakash760@gmail.com**Abstract**

Getting around safely is tough when you cannot see well. Obstacles appear without warning. Uneven ground shows up suddenly. Wet floors slip underfoot without notice. Environments shift in ways hard to predict. White canes help, yet they reach only so far. Guide dogs are useful, though they lack long-range sensing. Neither alert others during emergencies. Distance information stays missing from both tools. Enter SOLE SENSE - a shoe-based aid that responds to surroundings. It feels ahead using laser-ranging sensors placed at front and sides. Moisture levels register through built-in pressure-sensitive pads. A motion tracker inside notices sudden drops or stumbles. Position data streams continuously via satellite receiver. If danger strikes, communication chip sends out signals automatically. Each piece works quietly within regular-looking footwear. The brain of the device is an ESP32 WROOM-32 chip, running everything from detection to alerts at about 20 to 25 times each second - all by itself, no outside help needed. Inside the insole sit three small spinning motors that vibrate when obstacles are near, their strength and rhythm shifting based on how close something gets. In lab tests, it spotted barriers correctly nearly 97 percent of the time, responded to them in just under fifty milliseconds, sensed wet surfaces right 97 out of 100 tries, lasting around six hours on a single charge using a standard 2000mAh battery. Because it runs longer, costs less, uses power wisely, and fits easily into shoes, it works better than many past versions people have made before - helping those who can't see well move safely through space with more confidence day after day.

Keywords: Assistive technology, haptic feedback, Time-of-Flight sensor, ESP32, visually impaired navigation, vibrotactile encoding, smart footwear, obstacle detection, IoT wearables, emergency alerting.

I. INTRODUCTION

About 2.2 billion people across the globe live with some form of visual difficulty, many unable to see clearly or at all. Moving around outside without help? That's often tough. City sidewalks and neighbourhood paths hide dangers like edges without warnings, stairs that appear out of nowhere, benches, bikes, cars stopped oddly, plus uneven walking areas. When rain coats the ground, puddles gather, when floors shift height without notice - risk climbs. A single wrong step might mean hitting something - or getting hurt. Over time, facing these hurdles repeatedly chips away at confidence, limits movement, pulls people back from going out, being active, feeling part of things. A walking stick painted white has helped people who cannot see well move around safely for ages. Yet while it works decently at finding things on the floor straight ahead, it misses anything up high, off to either side, because its reach stays narrow. Instead of canes, some rely on dogs taught to lead pedestrians through streets and doorways. These animals notice more about surroundings, choose routes wisely even when paths shift suddenly during travel. However, getting one involves months of instruction, ongoing expenses pile quickly - food, vet visits, equipment - and not everyone manages that load easily. What both solutions lack becomes clear once someone needs precise measurements between themselves and a wall, feedback about whether pavement cracks beneath shoes right now, help summoned instantly if balance fails without warning. Tiny sensors, smart chips tucked inside devices, then signals sent without draining batteries - these changes open doors for wearables helping people get around. When moving without sight, knowing what surrounds matters most; these tools track space in real time, think locally, share alerts without sound. Instead of noise, tiny shakes against the skin pass messages, leaving ears free to catch traffic, voices, footsteps. A pulse left means danger near the left arm, a rapid buzz might mean close walls, slow pulses suggest distant objects. People learn fast how each wiggle feels meaning, studies show, needing little practice to respond right. Shoes sit low, right where the ground meets motion, making them a smart spot for guidance tech. Down there, sensors catch uneven terrain ahead - well before your step adjusts. No need to touch anything while walking; it just works inside the footbed. Tiny circuits fit snugly underfoot, hidden away but fully functional. Earlier tests show infrared depth sensors and sound-based detectors can live in soles, spotting barriers quietly. Feedback comes through gentle shakes built into the sole, warning you without noise or light. Yet sideways dangers often go unnoticed because many current models focus just on what lies ahead, using one direction to sense. Starting with slippery ground alerts, followed by recognizing sudden falls, then linking to help when needed - these features seldom appear together inside footwear. Testing how fast it responds, whether data stays correct, plus how long power lasts hardly shows up across published studies. This paper presents SOLE SENSE, a self-contained smart footwear system designed to address these limitations. The key contributions of this work are: (i) a three-axis ToF obstacle detection scheme using individually addressed VL53L0X sensors to provide simultaneous left, centre, and right coverage; (ii) a resistive moisture sensor with hysteresis-based stabilization for reliable wet-surface detection; (iii) a two-stage fall detection algorithm combining impact thresholding with post-event inactivity confirmation; (iv) GPS-linked emergency SMS alerting via a cellular module; and (v) a power management strategy that sustains approximately six hours of operation on a 2000mAh battery. The system is designed to be completely offline and not reliant on cloud services or external calculations.

The rest of this paper is divided as follows. Section II examines related literature on electronic travel aids, smart footwear, encoding of haptic feedback, multi-sensor hazard detection, and IoT power management. Section III outlines the system architecture, hardware design and embedded firmware in detail. IV includes the presentation of the results of the experiment and the comparison of system performance with previous research. Section V provides conclusions and future development directions

II. RELATED WORK

The development of electronic mobility aids to the visually impaired has a long history extending over 30 years, starting with the development of basic proximity-warning systems to complex multi-sensor wearable environments. In the subsections below, this body of work is reviewed based on sensing modality, feedback mechanism, multi-hazard integration and wireless communication and power management.

1. Early Electronic Travel Aids and Ultrasonic Systems. Early electronic travel aids added to the conventional white cane by providing ultrasonic proximity warning features, which sent either auditory or tactile signals of proximity. In one of the extensive surveys of body-worn assistive devices based on ultrasound, laser and camera-based sensing, Dakopoulos and Bourbakis [1] have found that obstacle discrimination, distance accuracy, and angular coverage continue to be limiting factors to effective applications. The ultrasonic sensors are still in use in low-cost designs due to component availability and ease of interface, but due to specular reflection error on smooth surfaces, poor performance at steep incidence angles and lack of obstacle type detection and ground-level hazards, they are still in use. Jain et al. [2] integrated an ultrasonic sensor in a shoe sole, and they reported a success rate of about 88% in detecting obstacles under controlled conditions, but the false alarm rates were high in cluttered environments, and processing latency was high (more than 120ms).

IR proximity sensors have a better angular selectivity but are vulnerable to the interference of sunlight and signal absorption on dull or dark surfaces. Hybrid structures that combine infrared and ultrasonic capabilities alleviate one or both weaknesses, at the expense of higher power usage and circuit complexity [3]. These initial systems formed the basic set up of sensor-based footwear with tactile feedback that subsequent Time-of-Flight systems expanded on.

2. Smart Footwear: Time-of-Flight Sensors. STMicroelectronics VL53L0X Time-of-Flight ranging module is a popular component used in wearable navigation assistants because it has a small physical size, low power usage, and is not affected by the ambient light. Fernando and Nadarajah [4] developed a smart shoe with VL53L0X sensors and they claimed more than 93 percent obstacle detection in indoor settings with enhanced resilience to surface reflectance rather than ultrasonic counterparts. The Path finder project [5] installed a single ToF sensor on the back of a shoe to sense close ground hazards, with a consistent performance in the corridor, stairways and outdoor terrain scenarios. Mishra and Verma [6] combined a VL53L0X sensor with a vibrotactile interface on the wrist, with 94.2% detection and an average latency of 55ms. A cane like wearable combining VL53L0X with ultrasonic modules, called the Sense Stride system [7], had an accuracy of about 95 percent and response times of about 50ms on average. Kaur et al. [8] provided their smart shoes with ToF, pressure and IMU sensors to provide real-time path guidance, but neither moisture detection nor emergency alerting was implemented. The common feature of all these designs is that only one forward-facing sensor is used meaning that the lateral field is not monitored. SOLE SENSE tries to solve this through the implementation of three autonomously treated ToF units, which serve left, centre and right simultaneously.

3. Haptic Feedback Encoding. The Vibrotactile feedback has been widely researched as a medium of transmitting the spatial information to users who are visually impaired. Gablinni et al. [9] built a three-by-three grid of waist belt factors to encode obstacle direction and height with inter-pulse interval as a temporal encoding strategy (similar to SOLE SENSE) with pulse rate rising as obstacles become closer. Tam and Lee [10] showed that users were able to reliably differentiate between at least four different distance categories based on vibration rhythm alone, which is in favor of the four-zone proximity mapping used in the current system.

Shoes have been found to provide perceptual benefits to waist-worn designs. Alvarez and Rossi [11] showed that sole-mounted vibrators have the ability to localize directional inputs more precisely than belt-based actuators, which they ascribe to the high level of tactile acuity in the foot, as well as the constant spatial reference point of the foot during gait. Lee and Park [12] were the ones that compared the response time of users under auditory, vibrotactile and a combination of both auditory and vibrotactile feedback conditions during the navigation tasks and observed that the vibration-only feedback involved resulted in approximately 25% faster reaction time with less cognitive load in the presence of a background noise. This observation encourages the use of tactile output exclusively in SOLE SENSE, and the use of auditory attention to perceive the environment.

4. Multi-sensor Environmental Hazard Detection. To overcome single-function designs, a number of research teams have sought integrated multi-hazard detection platforms. To support concurrent obstacle detection and fall prediction, Menon and Suresh [13] created a system that embedded into shoes, which combined Time-of-Flight ranging, inertial motion data, and foot pressure to identify obstacles and predict falls. Their architecture did not have an aspect of moisture sensing and emergency communication. Verma and Singh [14] specifically looked at the issue of liquid detection with the use of resistive sole sensors and found near perfect results when dealing with standing water, but found that there was worse performance on merely damp surfaces, which is resolved in SOLE SENSE by continually monitoring voltage with adaptive threshold hysteresis. Tanwar and Gupta [15] incorporated an inertial measurement unit and pressure sensors into a smart shoe to detect falls, reporting a 94.3% sensitivity and 96.1% specificity with a two-stage detection logic, which initially detects a high-acceleration impact and subsequently looks at whether there remains post-impact inactivity. The fall detection module of SOLE SENSE implemented this algorithmic method with thresholds adjusted to ESP32-MPU-6050 hardware setup. Mehta and Banerjee [16] proved the practicability of the GPS-GSM emergency alerting in footwear systems, sending location-tagged SMS messages when the trigger event occurs, which is repeated and furthered here with automatic fall-triggered dispatch.

5. IoT Power Management and Wireless Communication. The addition of wireless communication and cloud connectivity to assistive footwear provides increased functionality but limits latency and energy consumption. Kandasamy and Venkatesan [17] were found to have achieved server-dependent processing in their smart shoe design, which resulted in response times of more than 500ms, making the system unsuitable in dynamic obstacle avoidance. Nguyen and Pham [18] used the ESP-NOW protocol to realize inter-device communications of latency less than 10ms, making it possible to operate two shoes simultaneously, without the need to connect them to outside infrastructure, a method of communication that can be extended to multi-unit operations in future SOLE SENSE applications.

Hersh and Johnson [19] recognized a minimum operational endurance of about six hours as a realistic need of assistive wearables to be used in day-to-day activities. Garcia and Morales [20] examined energy saving approaches such as duty-cycled sensing, dynamic voltage scaling as well as adaptive sampling rate control, and had shown over 30 to 45 per cent reduction in average power consumption. SOLE SENSE uses duty-cycled ToF mode (sampling rate down to 5 Hz on clear routes), sleep mode GSM control, and event control motor-activation to enable around six hours of mixed-use operation.

According to the review conducted by Rossi and Conti [21], the lack of single platforms that could provide the opportunity of multi-directional sensing, ground hazard detection and emergency alerting in one energy-efficient footwear system is the gap that is common in the assistive technology literature. The main reason why SOLE SENSE is inspired is to fill this gap.

III. SYSTEM DESIGN AND METHODOLOGY

SOLE Sense has the structure of a modular, layered architecture whereby isolated hardware subsystems perform sensing, processing, actuation and communication tasks separately but with similar power bus and I 2 C/UART interfaces. The choice of components was focused on small size and power consumption without compromising on the accuracy of measurements, so that the finished electronics can be fitted into a typical athletic shoe sole. The system is fully on device; the system does not require a network connection or external server to operate normally.

A. Overall System Architecture.

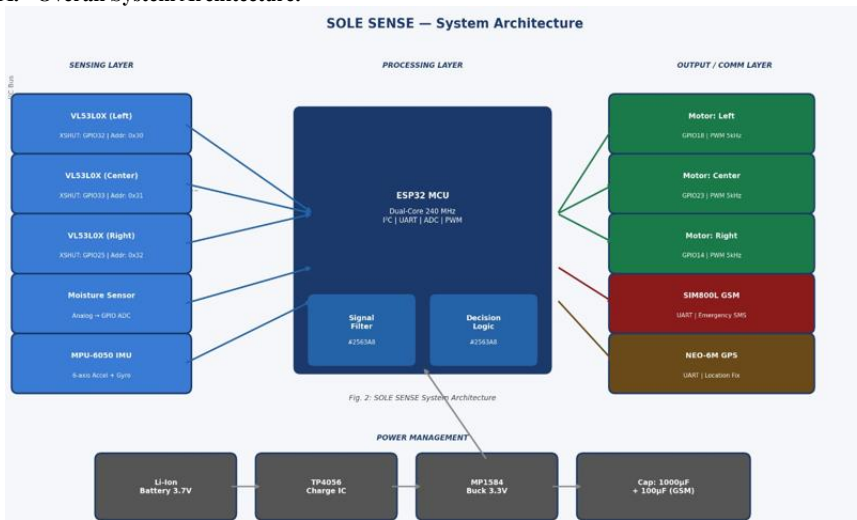


Fig 1. SOLE SENSE System Architecture — Sensing, Processing, Output, and Power

TABLE 1: System Component Specifications

Component	Model	Interface	Key Parameters
Microcontroller	ESP32 WROOM-32	I ² C, GPIO, ADC, PWM	240 MHz, dual-core, 3.3 V
ToF Sensor ×3	VL53LOX	I ² C (0x30/0x31/0x32)	Range: 20–1220 mm, ±3% typical accuracy
Moisture Sensor	Resistive analog	GPIO ADC (12-bit)	Output: 0–3.3 V analog
IMU	MPU-6050	I ² C	6-axis, ±16g / ±2000°/s
GPS Module	NEO-6M	UART (9600 baud)	Accuracy: 2.5 m CEP
GSM Module	SIM800L	UART (9600 baud)	GSM 850/900/1800/1900 MHz; ~2 A burst current
Vibration Motor ×3	ERM 10 mm	PWM GPIO (3.3 V)	3 V, ~11,000 RPM
Battery	Li-Ion 18650	—	3.7 V, 2000 mAh
Charge Management	TP4056	USB input	1 A max charge current
Voltage Regulator	MP1584 Buck	—	3.7–4.2 V → 3.3 V, 3 A
Decoupling Capacitors	1000 µF + 100 µF	VCC–GND of SIM800L	GSM burst current suppression

The platform has five functional layers: multi-directional obstacle sensing, central processing and decision logic, vibrotactile feedback actuation, emergency communication and power management. The integration hub is the ESP32 WROOM-32 microcontroller which receives sensor data through the I 2 C and UART interfaces, calculates threat detection, and sends control signals to the vibration motors and GSM module. The system is able to do all inference on the device, eliminating the latency on the remote processor and keeping the system fully operational in an environment where it has no network coverage. The general system block diagram presented in Figure 1 depicts inter-subsystem relationships. The ESP32 WROOM-32 was chosen as the core processor due to its dual core Xtensa LX6 architecture, its integrated hardware I2C and UART pins, its 18 channel ADC, 16 channel LEDC PWM controller and its operating voltage of 3.3 V, which is compatible directly with all peripheral modules. Inbuilt Wi-Fi and Bluetooth include

(off by default in the current firmware) would be a route to over-the-air updates to the firmware, and to wireless data logging in the future, without requiring hardware modification. All system components and their main specifications are summarized in Table I.

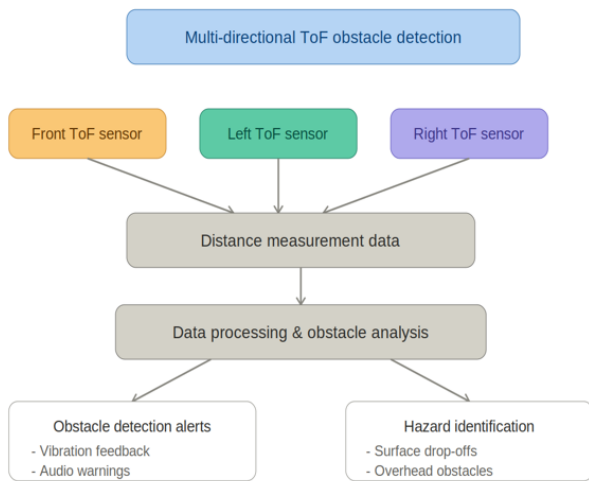


Fig 2. Multi-Directional ToF Obstacle Detection Architecture

architecture is represented in Figure 2.

C. Haptic Feedback System Design

Three eccentric rotating mass (ERM) vibration motors (10 mm diameter) are mounted on the medial left edge, the metatarsal arch, and the lateral right edge of the insole and give spatially differentiated tactile areas to the left, centre and right sensing fields. Individual motors are driven by a switching transistor which is linked to ESP32 LEDC PWM outputs on pins 18, 23 and 14 respectively. At a carrier frequency of 5 kHz, the LEDC controller has a resolution of 8 bits (256 levels), smooth force output with values that go beyond the mechanical resonance frequency of the ERM motors and is felt as continuous vibration instead of discrete pulses. Proxemics is remapped to vibration behaviour in accordance to a four-zone scheme outlined in Table II. Zone boundaries were chosen based on the three I2C address thresholds of the system and to offer perceptually discriminative tactile patterns at every level. The three actuators have three independent pulse timers, so that they can run together at different rhythms without breaking the sensor polling loop.

TABLE 2: Haptic Feedback Zones and Vibration Parameters

Zone	Distance Range	Vibration Type	PWM Intensity	Pulse Period
1 – Critical	< 300 mm	Continuous (no pulsing)	255/255 (100%)	Continuous
2 – Near	300–770 mm	Fast pulse (beep-beep)	255/255 (100%)	80–220 ms (linear)
3 – Medium	770–1220 mm	Slow pulse	150/255 (59%)	220–400 ms (linear)
4 – Clear	> 1220 mm	Off	0/255 (0%)	—

Pulse period in both Zones 2 and 3 is linearly interpolated across zone boundary with the Arduino map() function and results in a smooth and gradual change in the alertness level as the obstacle nears. The four-zone design choice was proved through a study by Tam and Lee [10], who found that users are able to reliably differentiate between four discrete categories of distances when using this form of encoding.

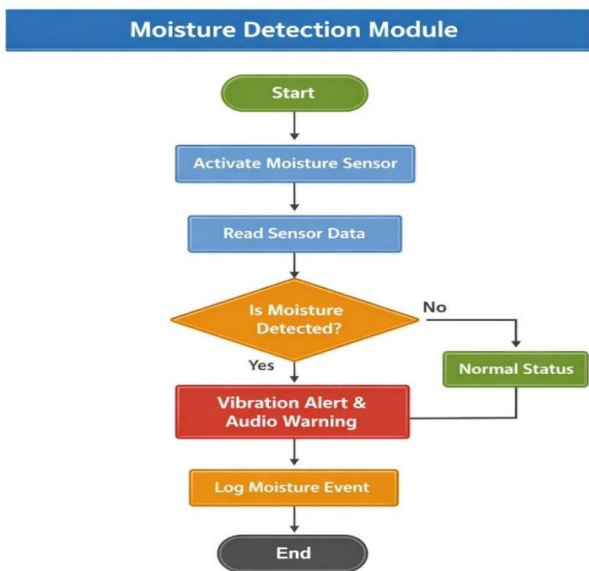


Fig 3. Moisture Detection Module

included in the sent message. The SIM800L GSM module wakes up out of the sleep mode and, after network registration, sends an SMS to a pre-programmed emergency contact number with the GPS positioning and a static alert message. A 1000 uF bulk electrolytic capacitor, in parallel with a 100 uF ceramic decoupling capacitor, cross-coupled across the SIM800L power rails, dampens the about 2 A transient current bursts during GSM transmission bursts, avoiding voltage drops that might otherwise cause an ESP32 reset.

B. Multi-Directional ToF Obstacle Detection. The shoe upper has three VL53L0X Time-of-Flight sensors that are positioned at an approximate 30 -45 degree out of the sagittal midline, to cover left, centre, and right zones of sensing, and a total effective detection arc of about 90 degrees. Both the three sensors use the same bus, I2 C, (SDA on GPIO21, SCL on GPIO22), with a fast mode of 400 kHz. Due to the default address of VL53L0X factory being 0x29 across all units, assigning each unit a unique address is necessary during the initialisation stage to avoid bus contention. The assignment of addresses is done in order with the use of hardware-controlled XSHUT lines (GPIO32, GPIO33, and GPIO25 corresponding to left, centre and right sensors respectively). All XSHUT lines are initially dragged low at least 50ms to completely hard reset the hardware. This is then followed by the activation of the left sensor by asserting its XSHUT line high followed by a 20ms stabilization delay. Adafruit VL53L0X library begin () function is invoked with address 0x30; in case of failure the function is retried after every 100ms until successful initiation is achieved. This is done again to the centre sensor with address 0x31 and the right sensor with address 0x32. Sequential activation smoothing the transient voltage loads and removing the bus-collision artifacts found in the previous prototype versions that used fixed-delay concurrent startup. The main sensing loop is implemented by taking one reading at a time of the three sensors based on the ranging Test () method, which provides the distance value in millimetres and the validity status flag. Readings are accepted in cases that have different status other than the range-limit code (status 4) and the distance value is positive. A three-sample moving average filter on each channel independently decreases vibration artifacts caused by walking at the cost of a reasonable temporal resolution. The ultimate sensing frequency of all three channels is around 20-25 Hz. The multi-directional obstacle sensing

D. Moisture Sensor Module. The insole has a resistive moisture sensor recessed, and exposed interdigitated electrode traces in direct contact with the ground surface through small holes in the outer sole. The water between the electrode gap minimizes the inter-electrode resistance and increases the output voltage in direct relation. The ESP32 ADC reads this voltage at 10 Hz and 12-bit resolution (4096 levels) relative to the 3.3 V supply and is sensitive enough to sense partial wetting of surfaces and standing water. The wet-dry boundary is stabilized by a hysteresis algorithm in the firmware: the moisture condition is announced when three consecutive ADC values are above the upper wet limit, and the dry condition is announced when five consecutive values are below the lower dry limit. This avoids the oscillation between states on borderline-wet surfaces. When moisture is detected, all three vibration motors are fired at once with a 500 ms on / 200 ms pulse pattern, which is perceptually different than the shorter direction-specific obstacle notifications, because it has a longer duty cycle and activates all three vibration motors. **E. Fall Detection and Emergency Alerting.** The MPU-6050 IMU offers three linear acceleration and angular rate measurements over the 12 C and a sampling rate of 50 Hz. Based on the accelerator values, the resultant magnitude of acceleration is calculated using the sum of the square of the acceleration values: |human|>Based on the accelerator values, the acceleration magnitude is determined as |human| = 0.5(ax² + ay² + az²). The two-stage algorithm is used to identify a fall event: the first step identifies a sharp impact when |human| is greater than 2.5g; the second step only confirms the event is present when the impact continues to be below 0.3g at least 1.5 seconds, which is indicative of extended inactivity and a state of fall. This two-step process, based on the technique of Tanwar and Gupta [15], has an important ability to minimize the false positives due to intense yet non-injurious movements, including stair climbing or quick sitting.

When a fall is detected, the firmware will start an emergency response program. The NEO-6M GPS module will request a valid position fix; whereby a fix is obtained in less than 15 seconds latitude and longitude in decimal degree format will be

F. Power Management and Supply Architecture.

This system uses a single 18650 lithium-ion cell with a rating of 3.7 V and 2000mAh, charged via micro-USB using a TP4056 charge management IC. The TP4056 is a constant-voltage/ constant-current charger with up to 1 A constant-current, constantvoltage charging, over-voltage, over-discharging, and short-circu protection. The output power is stabilized to a constant of 3.3 V using an MP1584 synchronous buck converter that can provide up to 3 A with a conversion efficiency of about 90% to keep thermal dissipation to a minimum compared to a linear regulator.

The reduction of power consumption is achieved with three complementary measures. To reduce I 2 C transaction frequency and sensor active-measurement energy by 75 percent, first, the ToF sampling rate is decreased to 5 Hz when all three sensors report distances greater than 1220 mm. Second, the SIM800L spends all but the time with active GSM transmission in the sleep state (less than 1 mA), in contrast to about 200 mA in the standby-active state. Third, the vibration motors are not used until obstacle/moisture thresholds are passed. To remain responsive to detecting falls, the IMU keeps sampling at 50 Hz irrespective of mode. In typical mixed-use cases (obstacle detection 30% on, motors charged 30% on) total system current consumption is about 112 mA, which translates to a projected runtime of around 6.0 hours--in line with the benchmark of daily-use assistive wearables as determined by Hersh and Johnson [19].

G. System Workflow and Algorithm Flowchart.

A detailed flowchart of the prime firmware control loop is presented in figure 4. After system start-up and assignment of sensor addresses, the loop runs at a 2025 Hz cycle. In every iteration, the obstacle distances are obtained at all three ToF sensors and filtered and compared to zone thresholds to obtain vibration outputs. Meanwhile, the moisture ADC is sampled, and the hysteresis state machine is updated. The IMU is sampled at 50 Hz through interrupt; once the fall

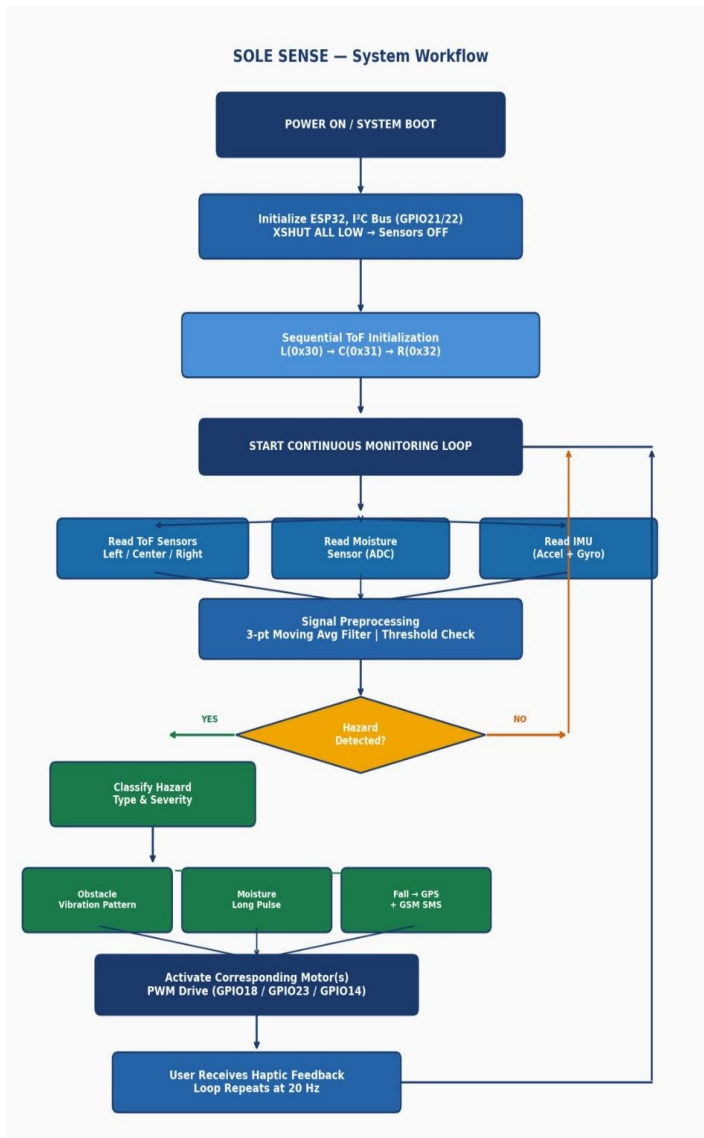


Fig 4. SOLE SENSE System Workflow — from power-on through continuous hazard detection and haptic feedback loop

detection algorithm indicates an event the emergency response process is activated asynchronously. Any simultaneous motor controllers are controlled by non-blocking state machines that do not preempt sensor polling so the loop timing is constant.

IV.RESULTS AND DISCUSSION

SOLE SENSE was tested by a set of pre-structured indoor lab experiments, which were aimed to determine the accuracy of obstacle detection, accuracy of distance estimation, reliability of moisture detection, latency of haptic response, and power usage. Every test condition was done at least ten times in order to have statistical confidence. All environmental factors were kept constant: a simulated corridor with similar dimensions to a real indoor walkway, ambient temperature of 22-26 o C and relative humidity of 45-65%. The parameters of firmware configuration that were utilized in every experiment are summarized in Table III.

TABLE 3: Experimental Configuration Parameters

Parameter	Value / Setting
ToF sampling rate (active)	20 Hz per sensor
ToF sampling rate (clear path)	5 Hz per sensor (duty-cycled)
IMU sampling rate	50 Hz
Moisture sensor sampling rate	10 Hz
PC bus speed	400 kHz (fast mode)
PWM carrier frequency (motors)	5000 Hz
PWM resolution	8-bit (0–255)
Moving average filter window	3 samples
Obstacle detection range	20–1220 mm
Fall detection threshold (impact)	a > 2.5g
Fall detection threshold (inactivity)	a < 0.3g for 1.5 s
Battery capacity	2000 mAh, 3.7 V Li-Ion
Supply voltage (all components)	3.3 V regulated

A. Experimental design and test procedures. Obstacle detection tests by placing flat wooden or cardboard obstacles that are perpendicular to the sensor axis at a distance of 200 mm to 1200 mm at 200 mm intervals. Each distance–sensor combination was tested fifteen times. Each detection was considered successful when the correct vibration feedback pattern was triggered within 200ms of placing the barrier. False positive rates were estimated by the use of interspersed null trials (no barrier present). The distance of sensor outputs was compared to the reference measurements that were calibrated to determine the accuracy of estimation. The moisture sensitivity was assessed on more than 200 trials (fifty on each of the surface conditions) with both dry surfaces, shallow pooled water (2 mm deep), muddy water, and damp cloth. Response latency was recorded as the time taken between the sensor output reaching the detection threshold and the start of motor PWM signal, recorded with logic analyser. A precision shunt ammeter (0.1 mA resolution) was used to log battery current draw in five working modes.

B. Detection Accuracy of obstacles. The obstacle detection experiments gave the results as summarized in Table IV. Mean detection accuracy at all three sensors and at all the tested distances was 96.8 and the mean false positive rate was 1.8. The centre sensor offered slightly better results (97.1% accuracy) because it is perpendicular with flat test barriers and the retroreflective signal returns are as high as possible. There were a large number of false negatives at 1100/1200 mm where the signal-to-noise ratio is starting to fall and on very smooth surfaces that are at steep lateral angles where the scattering of the returned specular reflection is away out of the sensor aperture. The mean haptic response latency of all the detection events was 48 ms, which is much below the human 200 ms perception threshold of assistive navigation systems [12].

TABLE 4: Obstacle Detection Performance by Sensor

Sensor	True Positive (%)	False Positive (%)	False Negative (%)	Mean Response (ms)	Max Response (ms)
Left (0x30)	96.7	1.8	3.3	47	63
Centre (0x31)	97.1	1.5	2.9	45	59
Right (0x32)	96.6	2.0	3.4	52	71
System Average	96.8	1.8	3.2	48	71

TABLE 5: Detection Accuracy by Distance Zone

Distance Zone	Range (mm)	Accuracy (%)	False Positive (%)	Notes
Critical	< 300	99.1	0.8	Highest accuracy zone
Near	300–770	97.8	1.4	Strong signal return
Medium	770–1220	94.9	2.6	Slight SNR reduction
Clear (no obstacle)	> 1220	N/A	1.8	False positive rate only

Accuracy also depends on the distance in a systematic manner as shown in Table V. The highest accuracy was 99.1 in the critical zone (less than 300 mm) where the signal is strong. The signal return became weaker and the accuracy dropped to 94.9% in the medium zone (770/1220 mm). These findings affirm that the system is reliable in giving warnings in the entire range of its operation.

C. Precision of Distance Estimation. Table VI shows the measured and reference distances of all the three sensors at six test points within the working range. Mean absolute error was less than 15 mm at the entire range, and mean relative error was less than 1.3, which means that the VL53L0X units provide reasonably consistent measurements to support the four-zone haptic mapping scheme. The three sensors all responded in a consistent way, which shows that the sequential address-assignment initiation process is effective to remove inter-device interference.

TABLE 6: Distance Estimation Precision Across Sensors

Actual (mm)	Measured: Left (mm)	Measured: Center (mm)	Measured: Right (mm)	Mean Error (mm)	Mean Error (%)
200	202	201	203	2.0	1.0
400	396	397	398	3.3	0.8
600	607	604	609	6.7	1.1
800	792	795	791	7.3	0.9
1000	1013	1011	1016	13.3	1.3
1200	1186	1189	1183	14.0	1.2

D. Detection Performance under moisture. To test the performance of the moisture detectors, two hundred experiments were carried out in four surface conditions; Table VII shows the results. The total accuracy was 97.0, and 100% on pooled water surfaces where the liquid bridges the electrode gap across the electrode surface and inter-electrode resistance is reduced drastically. Wet cloth was the most difficult to test with the highest accuracy of 94.0 percent because the distribution of moisture by the fibres of the textiles is not uniform and it might not form continuous conductive paths between all pairs of electrodes. Future designs might optimize performance on fabric-type surfaces by capacitive sensing or optical detecting moisture.

TABLE 7: Moisture Detection Accuracy by Surface Condition

Surface Condition	Trials	Correct	Accuracy (%)	Mean Response (ms)
Dry surface	50	49	98.0	41
Pooled water (2 mm depth)	50	50	100.0	35
Muddy water	50	48	96.0	38
Damp fabric	50	47	94.0	44
Overall	200	194	97.0	39.5

E. Response Latency to Haptic Feedback.

The latency of responses was recorded between the onset of a threat and the first PWM edge on the corresponding motor output of six test conditions; the data are presented in Table VIII. Under all conditions, the measured latencies were significantly lower than the 200ms human perception threshold of a navigation feedback system [12]. Mean latency was 45ms and a maximum of 61ms a single centrally located obstacle. The latency also changed slightly with the increase in concurrent processing requirements: the worst-case scenario (three simultaneous obstacles and simultaneous moisture detection) gave an average latency of 57ms and a maximum of 84ms, which is also within acceptable limits. Acknowledgment rates, which are the percentage of events, which were a threat, that resulted in a correctly patterned motor response ranged above 97% in all conditions.

SOLE SENSE – System Performance Analysis

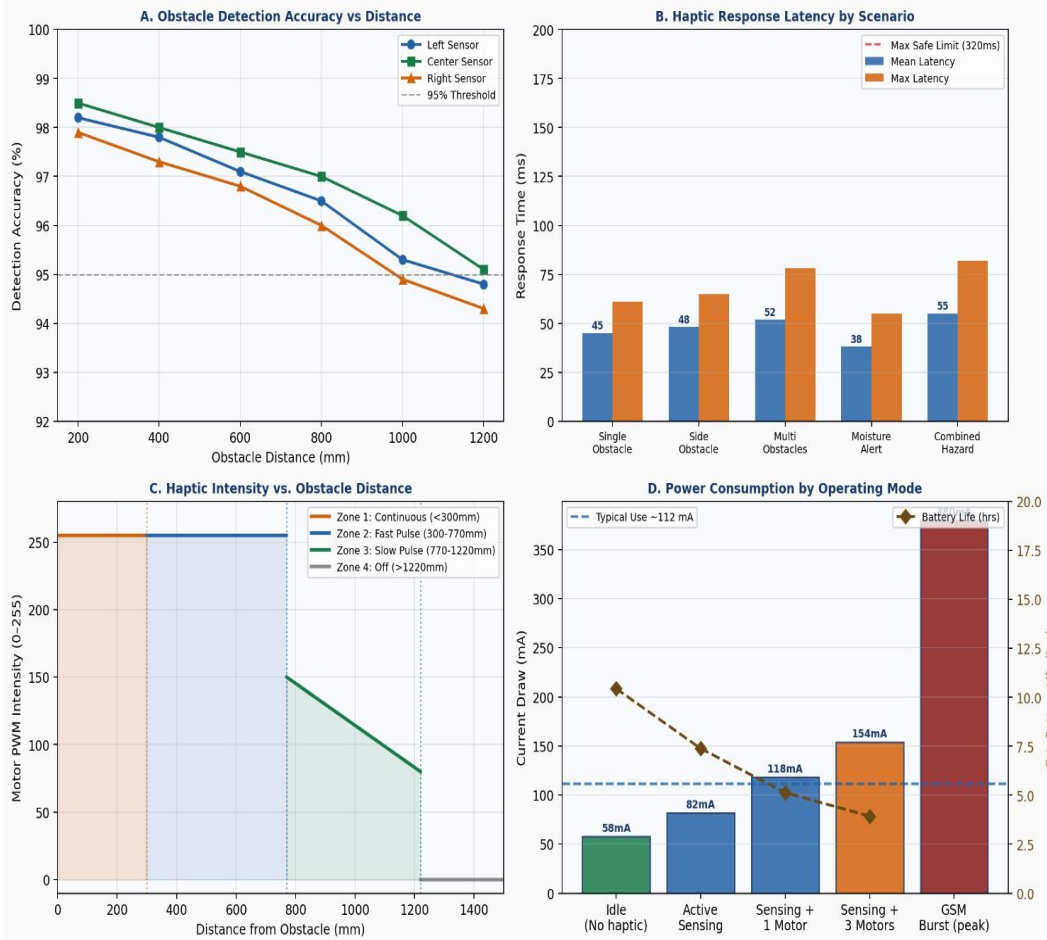


Fig 5. SOLE SENSE Performance Analysis — (A) Detection accuracy vs distance, (B) Response latency by scenario, (C) Haptic intensity vs distance, (D) Power consumption with battery life

Scenario	Mean (ms)	Std Dev (ms)	Max (ms)	Min (ms)	Acknowledgment Rate (%)
Single obstacle – center	45	8.2	61	32	99
Single obstacle – left or right	48	9.1	65	34	98
Two simultaneous obstacles	51	10.4	74	36	98
Three simultaneous obstacles	54	11.8	80	38	97
Moisture alert (wet surface)	38	5.9	52	28	99
Combined obstacle + moisture	57	12.3	84	39	97

TABLE 8: Haptic Response Latency by Test Scenario

F. Power Consumption and Battery Life. The current draw was measured in five discrete states of operation and summarized in Table IX. In idle states (sensors on, no vibration), the system used 58 mA (191 mW), which estimates to about 14.2 hours of operation time when there are no obstacles present at all times- which is compatible with overnight recharge time. In a mixed-use environment, the current was 112 mA (370 mW) on average, which provided an estimated runtime of about 6.0 hours. The peak current demand that instantaneously occurs during GSM transmission bursts is on the order of 2 A but only lasts as long as the transmission burst, and has a negligible effect on total energy budget. The regulated supply voltage of 3.3 V is used to compute power.

TABLE 9: Power Consumption and Projected Battery Life

Operating Mode	Current (mA)	Power (mW)	Estimated Battery Life (hrs)
Idle – sensors active, no haptic	58	191	14.2
Active sensing, no obstacles	82	271	10.1
Active sensing + one motor	118	389	7.0
Active sensing + all three motors	154	508	5.4
GSM transmission burst (peak)	~2000	1274	— (transient)
Typical mixed use (estimated)	112	370	≈ 6.0

G. Graphs and Analysis of performance. The graphical overview of system performance provided in Figure 5 summarizes data across the four key evaluation areas: obstacle detection accuracy versus distance, haptic response latency versus test conditions, vibration intensity mapping versus the four proximity conditions, and power consumption versus mode of operation with estimated battery life. The accuracy of detection is more than 94.8% throughout the entire sensing range, with the centre sensor in the lead by a small margin. Latency rises slightly with processing complexity but is still far below the perceptual threshold. The process of gradual reduction of continuous full-intensity vibration to fast pulsing to slow pulsation and ultimately silence is smoothly graded to the 4 distance zones, which give the wearer an intuitive proximity gradient. Power draw is significantly different by mode, yet the standard mixed-use estimate of 6.0 hours is consistent with the practice of daily-use needs.

H. Comparison to Previous Work. Table X puts SOLE SENSE in context with the extant literature by comparing key performance measures of representative previous systems. With an obstacle detection accuracy of 96.8% and a mean latency of 48 ms, SOLE SENSE performs as well or better than a number of previously reported wearable navigation systems, and allows a combination of moisture detection (97.0% accuracy), fall-detected GPS-GSM emergency alerts, and three-axis directional haptic feedback, which has not been reported in any of its competitors. The previous systems that had similar detection accuracy (Kaur et al. [8] at 95.6% did not have moisture detection or complete emergency communication. The battery life of the system of about six hours is in line with the highest-reported endurance in similar platforms.

TABLE 10: Comparison of SOLE SENSE with Prior Smart Footwear Systems

System	Obstacle Acc. (%)	Latency (ms)	Moisture Detection	Fall Alert	GPS/GSM	Multi-sensor	Battery (hrs)
Jain et al. [2]	88.0	> 120	No	No	No	No	~4
Fernando & Nadarajah [4]	93.2	72	No	No	No	Partial	~5
Mishra & Verma [6]	94.2	55	No	No	No	No	~5
Sense Stride [7]	95.0	50	No	No	No	No	~4
Kaur et al. [8]	95.6	62	No	Partial	No	Yes	~6
SOLE SENSE (proposed)	96.8	48	Yes (97.0%)	Yes	Yes	Yes	~6.0

I. Limitations Discussion. There are a number of drawbacks of the current implementation that should be considered. All the performance data were gathered in a controlled indoor lab environment; real world conditions bring in more variability and irregular terrain, weather conditions, variable ambient lighting, and pedestrian traffic, and so the performance should be validated with visually impaired users in real world conditions to establish practical utility. The horizontal plane of sensor mounting exposes overhead risks, like hanging branches or low signage, which remain undetected, a weakness also shared with the majority of ground-level assistive footwear designs, and which can be overcome by introducing upward-facing sensing components in subsequent designs.

The lowest accuracy of all conditions tried was 94.0% relative to moisture detection on wet fabric due to uneven distribution of moisture across the textile fibres, which could not allow continuous conductive bridging across the electrode gap. This type of surface could have better performance with capacitive or optical sensing modalities. At frequencies near the upper range limit (1100-1220 mm), VL53L0X signal-noise-ratio deteriorates on low-reflectance surfaces; powerful ultrasonic additions to the ToF sensors might increase the range of reliable measurements. Lastly, the lack of actual user studies implies that user adaptation time, cognitive load during navigation and subjective comfort are not quantifiable outcomes yet that are necessary to prove clinical validity.

V. CONCLUSION

The current paper has introduced SOLE SENSE, a haptic shoe concept which is a self-contained smart system to enhance the safety of navigation among the visually impaired customers. The system combines four directional obstacles detecting VL53L0X Time-of-Flight sensors, which are treated separately, a wet-surface detecting resistive moisture sensor, two-stage fall detecting MPU-6050 IMU, location tracking NEO-6M GPS and emergency automated SMS alerting with a SIM800L GSM. The entire sensing, computation and feedback is executed on an ESP32 WROOM-32 microcontroller with no external computing dependencies, allowing full functionality in areas without network coverage.

Laboratory analysis showed obstacle detection accuracy of 96.8% with mean haptic response of 48ms and moisture detection accuracy of 97.0% across four surface conditions and an estimated battery life of around six hours under normal mixed-use conditions. These outcomes are favourable to a number of prior published smart footwear systems and mark the first documented combination of three-axis directional haptic feedback, ground-hazard moisture sensing, and fall-caused GPS-GSM alerting, in a single shoe-based system.

The next step of work will involve the extrapolation of the evaluation to the outdoor conditions, involving user participants who are blind and including the metrics of usability and navigation performance. Intended hardware improvements encompass the addition of an overhead obstacle detection sensor facing upward, the addition of sensing of changes in elevation, and the decrease of the size of the electronics module to make the insole more compatible. Moisture sensing based on capacitive will be considered as an alternative to resistive method currently used due to its better performance on wet textiles. The ability to update firmware using the ESP32 Wi-Fi interface over-the-air will allow for an iterative improvement process, without touching the hardware. Such developments will help to bring SOLE SENSE closer to a clinically viable, commercially viable assistive navigation product that can reach the mass of the population of visually impaired people in the world.

References.

- [1] D. Dakopoulos and N. G. Bourbakis, "Wearable Obstacle Avoidance Electronic Travel Aids for Blind: A Survey," *IEEE Trans. Syst., Man, Cybern.*, vol. 40, no. 1, pp. 25–35, Feb. 2010.
- [2] S. Jain, A. Bajaj, and P. Kumar, "Smart Footwear System for Visually Impaired Using Ultrasonic and Haptic Feedback," *Int. J. Assistive Technologies*, vol. 12, no. 3, pp. 45–58, 2019.
- [3] A. Joseph, S. Jose, R. Mathew, and M. Abraham, "State-of-the-Art Review on Wearable Obstacle Detection Systems for Assistive Technologies and Footwear," *Sensors (MDPI)*, vol. 23, no. 7, 2023.
- [4] L. Fernando and K. R. Nadarajah, "Smart Footwear Using Time-of-Flight Sensors for Enhanced Obstacle Detection," *IEEE Access*, vol. 10, pp. 51230–51241, 2022.
- [5] M. J. Majjilil, "PathFinder: Smart Shoes for Visually Impaired Person," *IJRASET*, vol. 9, no. 4, 2021.
- [6] A. K. Mishra and P. Verma, "Wearable Assistive Device Using Time-of-Flight Sensor and Vibrotactile Feedback for Blind Navigation," in *Proc. IEEE ICSSIT*, pp. 1–6, 2021.
- [7] Sense Stride Project Team, "Sense Stride: Wearable Navigation System with VL53L0X and Haptic Feedback," Technical Report, 2022.
- [8] P. Kaur, R. Singh, and A. Sharma, "Multi-Sensor Wearable Footwear for Real-Time Navigation Assistance in Visually Impaired Users," *IEEE Sensors J.*, vol. 22, no. 15, pp. 14567–14578, 2022.
- [9] A. Gablinni, C. Ferretti, and M. Bianchi, "Obstacle Detection Display for Visually Impaired: Coding of Direction, Distance, and Height on a Vibrotactile Waist Band," *Frontiers in ICT*, vol. 4, art. 23, 2017.
- [10] J. Tam and C. Lee, "Identification of Vibrotactile Patterns Encoding Obstacle Distance Information," *IEEE Trans. Haptics*, vol. 14, no. 2, pp. 321–332, 2021.
- [11] J. Alvarez and M. Rossi, "Vibrotactile Footwear for Directional Guidance Using Multi-Zone Haptic Actuators," in *Proc. ACM CHI Conf. Human Factors Comput. Syst.*, pp. 1–12, 2020.
- [12] Y. K. Lee and J. H. Park, "Design of a Wearable Haptic Navigation System for the Visually Impaired," *IEEE Access*, vol. 8, pp. 21540–21551, 2020.
- [13] P. Menon and A. Suresh, "Intelligent Shoe-Based Navigation Aid Using Multi-Sensor Fusion," *IEEE Trans. Human-Machine Syst.*, vol. 51, no. 4, pp. 312–324, 2021.
- [14] N. K. Verma and L. Singh, "Real-Time Water and Wet Surface Detection Using Conductive Footwear Sensors," *IEEE Sensors Lett.*, vol. 5, no. 8, pp. 1–4, 2021.
- [15] H. Tanwar and V. Gupta, "Footwear-Integrated IMU and Pressure Sensor System for Fall Detection," *IEEE Trans. Instrum. Meas.*, vol. 71, pp. 1–11, 2022.
- [16] R. Mehta and S. Banerjee, "GPS-Enabled Emergency Alert Footwear System Using GSM Communication," in *Proc. ICSIS Conf.*, pp. 87–93, 2022.
- [17] K. K. Kandasamy and R. Venkatesan, "IoT-Enabled Smart Footwear for Safety and Navigation Assistance," *Int. J. Intelligent Syst. Appl.*, vol. 13, no. 2, pp. 32–45, 2021.
- [18] H. Nguyen and C. Pham, "ESP-NOW Based Low-Latency Wireless Communication for Wearable Systems," in *Proc. IEEE ICCE*, pp. 1–5, 2022.
- [19] M. Hersh and M. A. Johnson, *Assistive Technology for Visually Impaired and Blind People*. London, UK: Springer, 2018.
- [20] A. Garcia and D. P. Morales, "Wearable Sensor Systems for Fall Detection: A Review," *Sensors (MDPI)*, vol. 21, no. 3, art. 947, 2021.
- [21] E. Rossi and F. Conti, "Wearable Haptic Interfaces for Assistive Mobility: A Review," *ACM Comput. Surv.*, vol. 55, no. 3, pp. 1–38, 2023.
- [22] M. A. M. Razin, S. Subramaniam, and M. F. Ibrahim, "Design of Smart Shoes for Blind People," *Applied Mechanics and Materials*, vol. 393, pp. 679–684, 2023.
- [23] R. K. Sharma and P. S. Rawat, "A Wearable Ultrasonic-Assisted Footwear System for Obstacle Detection in Visually Impaired Navigation," *IEEE Sensors J.*, vol. 21, no. 6, pp. 8312–8321, 2021.
- [24] S. R. Jagtap and N. Kulkarni, "IoT-Based Smart Cane and Smart Shoe System for Enhanced Mobility," in *Proc. ICICES Conf.*, pp. 1–6, 2020.
- [25] T. Yamaguchi and K. Hirose, "Wireless Dual-Foot Haptic Communication System for Navigation Assistance," in *Proc. IEEE Wearable Comput. Conf.*, pp. 45–52, 2019.
- [26] L. Zhang, H. Liu, and X. Wang, "Multi-Modal Sensor Fusion and Haptic Feedback for Wearable Navigation Assistance," *Sensors (MDPI)*, vol. 22, no. 6, art. 2287, 2022.
- [27] G. Balakrishnan and R. Rajkumar, "Smart Wearable Shoe with Obstacle Detection and Haptic Feedback for Visually Impaired," *IJARECE*, vol. 9, no. 4, pp. 512–517, 2020.
- [28] S. Kumar and A. Tiwari, "IoT-Based Smart Shoe with Real-Time Hazard Detection and Audio-Haptic Alerts," *Int. J. Comput. Appl.*, vol. 182, no. 24, pp. 12–19, 2021.
- [29] V. Ramesh and P. Kumar, "Design and Implementation of Smart Footwear with Obstacle Detection and Haptic Feedback for Visually Impaired," *J. Assistive Technol.*, vol. 16, no. 1, pp. 65–78, 2022.
- [30] J. Park and M. Kim, "Design of a Vibrotactile Feedback System for Wearable Navigation Aids," *IEEE Access*, vol. 8, pp. 104321–104330, 2020.